Nondestructive Real-Time Measurement of Charge and Spin Dynamics of Photoelectrons in a Double Quantum Dot

T. Fujita,[1,*] H. Kiyama,[1] K. Morimoto,[1] S. Teraoka,[1] G. Allison,[1,2] A. Ludwig,[3] A. D. Wieck,[3] A. Oiwa,[1] and S. Tarucha[1,4]

[1]*Department of Applied Physics, The University of Tokyo, 7-3-1 Hongo, Bunkyo-ku, Tokyo 113-8656, Japan*

[2]*Department of Physics, Princeton University, Princeton, New Jersey 08544, USA*

[3]*Lehrstuhl für Angewandte Festkörperphysik, Ruhr-Universität Bochum, Universitätsstraße 150, Gebäude NB, D-44780 Bochum, Germany*

[4]*Center for Emergent Matter Science (CEMS), RIKEN, 2-1 Hirosawa, Wako-shi, Saitama 351-0198, Japan*

(Received 11 November 2012; published 25 June 2013)

We demonstrate one and two photoelectron trapping and the subsequent dynamics associated with interdot transfer in double quantum dots over a time scale much shorter than the typical spin lifetime. Identification of photoelectron trapping is achieved via resonant interdot tunneling of the photoelectrons in the excited states. The interdot transfer enables detection of single photoelectrons in a nondestructive manner. When two photoelectrons are trapped at almost the same time we observed that the interdot resonant tunneling is strongly affected by the Coulomb interaction between the electrons. Finally the influence of the two-electron singlet-triplet state hybridization has been detected using the interdot tunneling of a photoelectron.

DOI: 10.1103/PhysRevLett.110.266803 PACS numbers: 73.63.Kv, 03.67.Hk, 73.23.Hk, 72.25.Fe

The transfer of quantum information between single photons and solid-state quanta such as charge, electron spin, and nuclear spin has been extensively studied because it is an essential element towards the establishment of a global quantum information network. Semiconductor quantum dots (QDs) can be key systems for photon-electron quantum coupling since charge and spin qubit states along with their gate operations are both optically and electrically accessible [1–5]. Additionally, both photon polarization and electron spin are robust quantum states [6]. Preliminary experiments of information transfer between ensembles of these two quantum media have been performed in GaAs quantum wells [7,8]. Recently, the entanglement between photons emitted from a QD and spin in the QD has been reported in InAs self-assembled QDs [9–11].

To date several single photoelectron trapping experiments were performed in gate defined GaAs single QDs with a nearby charge sensor [1,2,12,13]. Single photoelectron spin states were also distinguished destructively using edge states [2]. Other schemes using the Zeeman effect or spin singlet and triplet states are feasible [6,14]. Spin measurement in single QDs is, however, usually destructive in the sense that the photoelectrons are immediately lost to the electron reservoir. Nondestructive transfer between separate dots is required to integrate a photon to spin conversion interface in quantum circuits. Double QDs (DQDs) provide a robust single spin readout through Pauli spin blockade.

The scheme of the quantum repeater based on coherent transfer using quantum-dot spins [15] may be achieved by the following process. Two photons from different entangled photon sources have to be captured in the same double quantum dot. They then must be entangled together without destroying quantum information using a two-qubit gate operation. Therefore, the nondestructive detection of two or more photoelectrons and their spin states using an electrically defined DQD, where the two qubit gate operation has been already realized [5], is a truly indispensable ingredient for a long distance entanglement distribution.

In this Letter, we use GaAs DQDs to study one and two photoelectron trapping and the subsequent nonequilibrium electron charge and spin dynamics. We find that it is feasible to probe the optically pumped electron by setting the two excited states of the dots on resonance and measuring the real-time interdot tunneling of the photogenerated electron in a nondestructive manner. This temporal response is observed within a few ms, much shorter, or at least comparable with the spin lifetime of $T_1 = 0.1$ to 1 sec at low magnetic fields [16]. Indeed, the spin dynamics of the single photoelectrons affected by the nuclear spins has been observed using the interdot detection scheme combined with the Pauli spin blockade. When more than one photoelectron were trapped at the same time within our time resolution, we have observed that the dynamics in the DQD is influenced by the Coulomb interaction. This would enable one to investigate the nonequilibrium multielectron dynamics inaccessible by the conventional all electrical transport measurements.

A two-dimensional electron gas (2DEG) formed at an n-AlGaAs/GaAs heterostructure or a quantum well (QW) wafer with well width of 7.5 nm is confined as a gate defined lateral DQD [Fig. 1(a)]. The QW wafer was used only for the photoelectron spin blockade measurements and has no essential difference from the single heterostructure within the discussion of this Letter. The electron temperature was 750 mK inside a ^{3}He cryostat with an

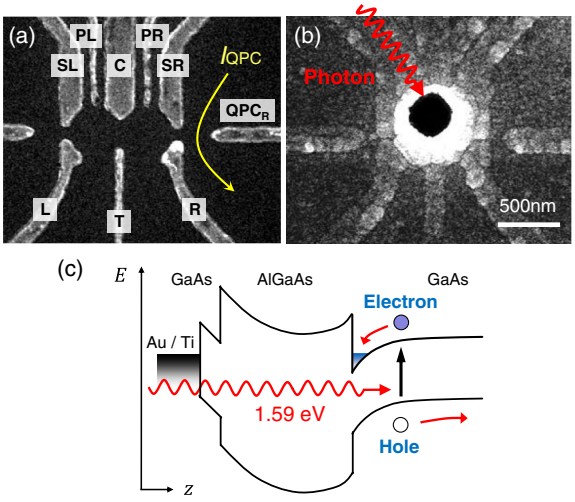

FIG. 1 (color online). (a) A scanning electron micrograph of the typical lateral DQD device. The surface gates for dot formation have Ti(10 nm)/Au(20 nm) metal thickness. A 60 nm thick Al_2O_3 insulating layer was formed on top of them by atomic layer deposition. (b) A Ti(30 nm)/Au(220 nm) mask was fabricated on the surface above the DQD with an aperture of 400 nm diameter. (c) Band profile of the HEMT structure. The excitation laser energy is tuned just above the GaAs band gap. The excited electron-hole pair is separated due to the intrinsic electric field.

optical window. A 30×30 μm^2 wide and 200 nm thick metal mask with a 400 nm diameter aperture is fabricated on top of the double dot to facilitate selective irradiation of the DQDs [Fig. 1(b)]. The transmittance through this aperture reaching the GaAs buffer layer is calculated as approximately $1/3$ using finite-difference time domain calculation [17]. A picosecond pulsed laser diode with the photon energy of 1.59 eV, which is slightly above the bulk GaAs band gap, is used to excite electron-hole pairs. Photons are mainly absorbed in the GaAs buffer layer under the DQD and the built-in electric field of the heterostructure separates the electron and hole and drives the electron into the DQD, which may result in a single photogenerated electron trapping in the dot [Fig. 1(c)].

The charge states in the DQD were measured with a quantum point contact [QPC_R, see Fig. 1(a)] charge sensor which has sufficiently higher sensitivity to changes of the right dot charge occupation compared to the left. The electron numbers were counted by analyzing the QPC transconductance $G_{QPC} = dI_{QPC}/dV_L$, where I_{QPC} is the QPC current and V_L is the voltage applied to gate L, using a lock-in technique with a modulation frequency of $f_m = 223$ Hz [Fig. 2(a)]. The (0,0) state was confirmed by applying sufficiently large negative voltage to the gates to ensure that no further lines appeared. The tunneling rates were then lowered so that real-time charge transitions were measurable. Tunneling rates between the dots and lead, and between the two dots were decreased to less than the bandwidth of our setup (3.3 kHz). The QPC sensitivities

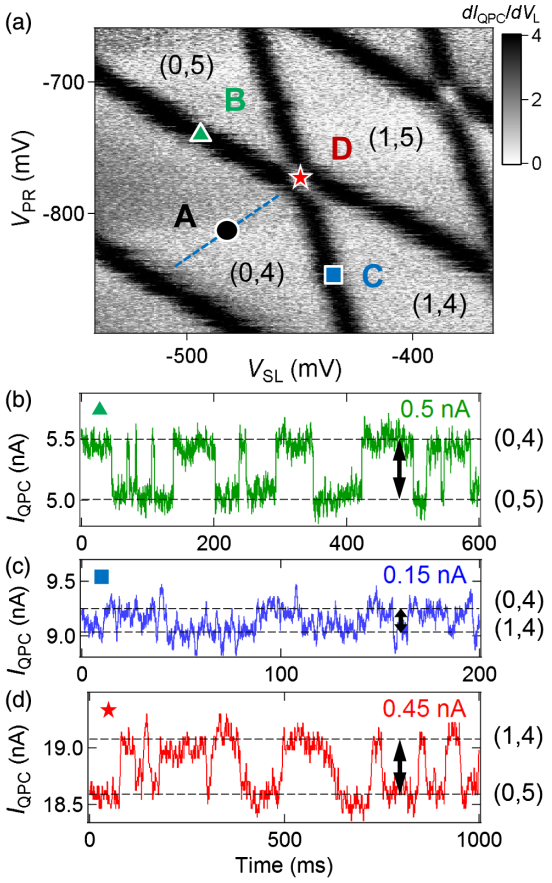

FIG. 2 (color online). (a) Stability diagram of the DQD. The dot was initialized to state A(0,4) before light irradiation. (b)–(d) Real-time charge sensing traces of the DQD measured at the resonance points B(0,4)-(0,5), C(1,4)-(0,4), and D(1,4)-(0,5). The 0.5 nA step height in (d) indicates the interdot tunneling event of a single electron charge.

were $2.5\% \times e^2/h$ [0.5 nA in Fig. 2(b)] for tunneling between the right dot and the lead, $0.5\% \times e^2/h$ for tunneling between the left dot and the lead [0.15 nA in Fig. 2(c)], and $2.0\% \times e^2/h$ for the interdot tunneling [0.45 nA in Fig. 2(d)]. Note that only the QPC sensitivity for the interdot tunneling is important in this study.

Before laser irradiation, the tunneling rate of the left (right) barrier was tuned to $\Gamma_L \approx 0.1$ Hz ($\Gamma_R \approx 1$ Hz). The interdot tunneling rate was adjusted ranging from $\Gamma_C = 10$ Hz to 1 kHz. The state that we will discuss is drawn schematically in Fig. 3(b). The initial charge state was set in the center of the (0,4) blockade region [(**A**) in Fig. 2(a)]. Here the ground state is (0,4) and the excited states (1,4) and (0,5) are energetically aligned. Therefore, when a single photoelectron relaxes into the DQD the charge numbers will be either (1,4) or (0,5). Since these two states are degenerate, interdot tunneling will be governed by the previously adjusted rate.

Figure 3(a) shows the temporal I_{QPC} data of single photoelectron trapping. Upon single laser pulse irradiation

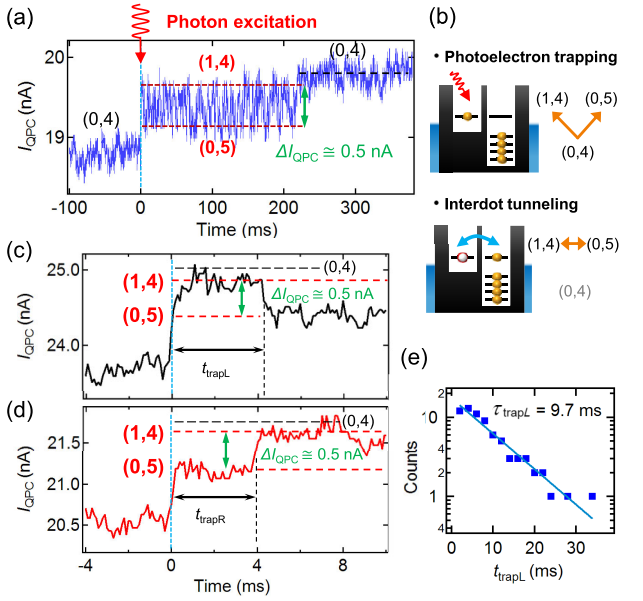

FIG. 3 (color online). (a) Single photon detection signal observed over a time scale much longer than the interdot tunneling rate. A fluctuation in the current is seen when a single extra charge tunnels between the two dots. At $t = 220$ ms, the electron escapes from the dot and the current returns to the value indicating the (0,4) state. (b) A schematic picture of the charge number during interdot tunneling of a photogenerated electron. (c) Measured sensor current upon pulse irradiation indicating interdot tunneling of a single photogenerated electron initially trapped in the left dot. (d) Interdot tunneling of a single photogenerated electron initially trapped in the right dot. (e) Histogram of t_{trapL}. Data were taken at the condition of an average thermal electron interdot tunneling time of 10.8 ms. The fitting time constant was $\tau_{trapL} = 9.7$ ms.

at time $t = 0$ the I_{QPC} abruptly increases and simultaneously starts to oscillate between two levels 0.5 nA apart. Then, it becomes constant at a current 0.15 nA higher than the top level. The final I_{QPC} after 220 ms is about 1 nA larger than that before the photon irradiation. A similar background increase was observed with the same pulses when no photon was trapped in the DQD. This is persistent photoconductivity induced by photon irradiation of the 2DEG near the QPC outside the metal mask. The temporal change of I_{QPC} in Fig. 3(a) is well understood by referring to each signal amplitude in Figs. 2(b) to 2(d) and each tunneling rate that was previously set. The first increase in the current is the addition of the persistent photoconductivity and the signal of an electron trapped in the far side left dot which forms a (1,4) excited state. The subsequent oscillating signal is the interdot tunneling of the photogenerated electron between the (1,4) and (0,5) resonant states. Such real-time observation of the resonant interdot tunneling has never been reported to the best of our knowledge. In the end, the dot is initialized to (0,4) when the electron escapes from the left dot to the lead. Note that the I_{QPC} fluctuation due to resonant tunneling between $t = 0$ and t_{trap} is clearly larger than the fluctuation of I_{QPC} for $t < 0$ before the light irradiation and for $t > t_{trap}$ after the escape of the photogenerated electron to the leads.

Single photoelectrons can be trapped by either dot because the aperture covers both dots. Figures 3(c) and 3(d) are magnified plots of I_{QPC} showing the single photoelectron trapping by the left dot Fig. 3(c) and by the right dot Fig. 3(d), respectively, immediately after the photon irradiation. Following the initial step of I_{QPC}, upon photon irradiation we observe an abrupt decrease of I_{QPC} by 0.5 nA at $t_{trapL} = 4.1$ ms in Fig. 3(c) but an abrupt I_{QPC} increase by 0.5 nA at $t_{trapR} = 4$ ms in Fig. 3(d). The I_{QPC} change is almost the same as observed in Fig. 2(d); therefore, the former is assigned to the charge state change from (1,4) to (0,5) and the latter to that from (0,5) to (1,4).

Next we confirm that the measured t_{trap} values are due to the photoelectrons trapped in the DQD and not due to any electrons entering from the 2DEG contact leads. Figure 3(e) is a histogram of measurements showing the same feature as Fig. 3(c) as a function of the extracted t_{trapL}. The decay time constant of $\tau_{trapL} = 9.7$ ms, obtained by numerical fitting of an exponential curve, is consistent with the average interdot tunneling time of 10.8 ms for a thermal electron. The decay constant obtained for measurements of the type of Fig. 3(d) also agrees with the tunneling rate of thermal electrons as measured in advance. These results are convincing because electrons from the reservoir would have tunneling times a few orders of magnitude longer.

To negate the effects of persistent photocurrent, we irradiated the sample using an infrared laser diode. This irradiation efficiently reduces the photoinduced carrier density in the 2DEG and therefore, the photoconductivity [18].

Use of the interdot resonant tunneling can raise the fidelity of single photoelectron trapping because it gives distinct evidence of trapping of single photoelectrons by either dot and also because the large resonant fluctuation of I_{QPC} makes it easier to distinguish the photoelectron trapping event from the background noise. In addition, resonant tunneling may be useful for spin detection of photogenerated electrons in DQDs with Pauli spin blockade, because the interdot tunneling is only allowed for the spin-conserving states between the dots.

Here, we show trapping and dynamics of two photoelectrons in a DQD. Figures 4(a) and 4(b) show two typical I_{QPC} traces for trapping of two photogenerated electrons by the DQD and their subsequent dynamics affected by the Coulomb interaction. The experimental condition is the same as used before, but the detection rates are much lower than those in Figs. 3(c) and 3(d). The resonant fluctuation of I_{QPC} only appears following an intermediate step after the laser pulse irradiation. By considering that I_{QPC} is more largely reduced by charging of the right dot than that of the left dot, the higher step relative to the initial (0,4) current

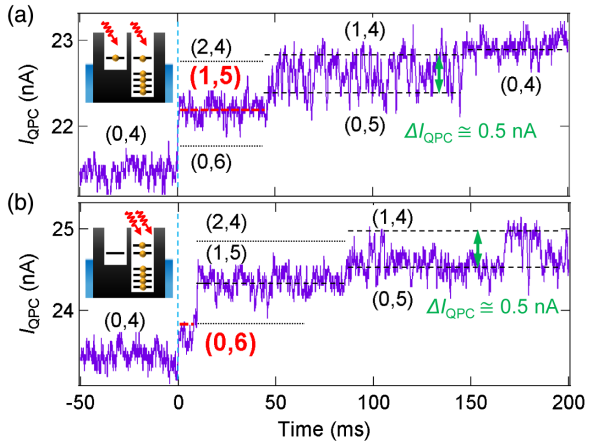

FIG. 4 (color online). (a) Signal indicating two photon detection. After the irradiation, two photoelectrons fill each QD at the same time. The sensor current is stable until one of the two photogenerated electrons escapes from the DQD. (b) Signal when two photogenerated electrons were trapped both in the right dot.

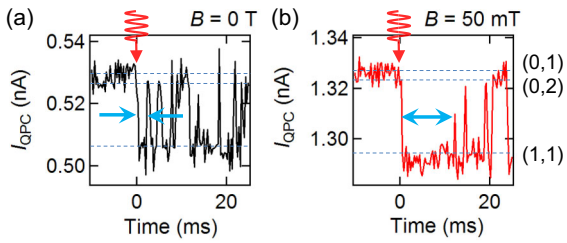

FIG. 5 (color online). Single photoelectron trapping in (0,1) initialized charge state with (1,1)-(0,2) excited states on resonance measured at (a) 0 T and (b) 50 mT. Photoelectrons are initially trapped in the left dot and resonantly tunnel into the right dot after 2.3 ms and 12.0 ms, respectively. The elongated tunneling time at finite magnetic field indicates the observation of electrons with parallel spin excited into the spin blockade configuration.

level in Fig. 4(a) is assigned to the (1,5) state and the lower step in Fig. 4(b) to the (0,6) state, respectively. We have found that the resonant interdot tunneling of photogenerated electrons is prevented due to the Coulomb interaction when each dot is occupied by a photogenerated electron and as soon as one of the two photogenerated electrons tunnels off the DQD, the resonant tunneling is resumed. Moreover, the trapping of two photoelectrons suggests that our scheme provides a way to initialize nonequilibrium multielectron states in gate-defined DQDs within an optical pulse duration. Such fast initialization is not feasible by electrical pumping because loading electrons from the leads connected to QDs through tunnel barriers is stochastic. In principle, the injection of more than two electrons is also feasible by optical means. Note that the two photoelectron trappings are distinguished owing to the large sensitivity difference between the two dots. Higher photon numbers may also be distinguished. In other words, the spectroscopy of higher energy states is possible by injecting many photoelectrons.

Here, we discuss the detection rates of zero, one, and two photoelectron trapping. 595 single pulses were irradiated with an average photon flux of 1.03 photons per pulse through the aperture above the DQD. Each signal was classified into either type shown in Figs. 3(c) and 3(d), or Figs. 4(a) and 4(b). The trapping rates were 14.1%, 19.3%, and 2.7%, respectively. (We eliminated dark counts with only one increase step of I_{QPC} after irradiation, which are presumably due to additional impurity levels nearby the QPC that also traps photoelectrons [17].) The features correspond to photon detection on the left dot, the right dot, and two or more photon detections. The average number of photons detected per incident pulse was 0.39 photons. This gives a trapping efficiency of 38% which is approximately a factor of two more efficient than we previously obtained for a single dot [2]. This may be due to a larger capture area for the photoelectrons created by light diffracted at the metal aperture and scattered in the buffer layer during the trapping process.

Finally, we show that the scheme for detecting the resonant interdot tunneling of photoelectrons can be used to extract its spin information. Figures 5(a) and 5(b) show the typical single photoelectron trapping signals by irradiating linearly polarized photons in a (0,1) initialized charge state with (1,1)-(0,2) excited states on resonance measured in a different sample. Figure 5(a) was measured at 0 T and Fig. 5(b) at 50 mT. In both measurements, a single photoelectron was initially trapped in the left dot seen as a 30 pA decrease step at 0 ms. In Fig. 5(b), the first resonant tunneling to the right dot appears at 12.0 ms whereas resonant tunneling instantly appears in Fig. 5(a). The longer time before a resonant tunneling event is seen indicates that the blockade of the photoelectron spin in the left dot parallel to the prepared electron spin in the right is instantly established and lifted after T_1. The lifetime of the blockade is determined by the hyperfine interaction with nuclear spins [19]. This result shows that our time scale used to resolve the real-time interdot tunneling events is also fast enough to follow the spin dynamics of photoelectron spins.

In summary, we demonstrated the trapping of single photons and interdot tunneling of the photogenerated electrons in a nondestructive manner using double quantum dots. The interdot tunneling time we observed was much shorter than the spin lifetime. When combined with Pauli spin blockade, projection measurements of the transferred photoelectron spin states is realized. We found that the interdot resonance is a robust method to identify single photoelectron trapping events, to discriminate the number of trapped photoelectrons and to detect photoelectron spin states. Our scheme offers a novel method to study the multielectron dynamics which are strongly affected by

the Coulomb interaction in a multidot system. Analogous to optical spectroscopy, the demonstrated results can be regarded as excited state spectroscopy. The fast initialization of the excited states such as fully spin-polarized multielectron states, that are not accessible by the conventional electrical pumping, can be realized by controlling the incident photon number, energy, and polarization. Also by appropriately designing the DQDs, this technique would open a way to high fidelity photon counting as well as nondestructive single photoelectron spin detection and storage.

This work was supported by Grants-in-Aid for Scientific Research S (No. 19104007) and A (No. 21244046 and No. 25246005), Innovative area (Grant No. 21102003), FIRST program, QuEST Grant No. (HR-001-09-1-0007), IARPA, MEXT Project for Developing Innovation Systems, and QPEC, The University of Tokyo. T. F. & H. K. are supported by JSPS Research Fellowships for Young Scientists. A. L. and A. D. W. acknowledge gratefully support from DFG-SPP1285, BMBF QuaHL-Rep 01BQ1035, and DFH/UFA CDFA-05-06.

*fujita@meso.t.u-tokyo.ac.jp

[1] M. Kuwahara, T. Kutsuwa, K. Ono, and H. Kosaka, Appl. Phys. Lett. **96**, 163107 (2010).
[2] A. Pioda, E. Totoki, H. Kiyama, T. Fujita, G. Allison, T. Asayama, A. Oiwa, and S. Tarucha, Phys. Rev. Lett. **106**, 146804 (2011).
[3] T. D. Ladd, F. Jelezko, R. Laflamme, Y. Nakamura, C. Monroe, and J. L. O' Brien, Nature (London) **464**, 45 (2010).
[4] K. C. Nowack, F. H. L. Koppens, Yu. V. Nazarov, and L. M. K. Vandersypen, Science **318**, 1430 (2007).
[5] R. Brunner, Y.-S. Shin, T. Obata, M. Pioro-Ladrière, T. Kubo, K. Yoshida, T. Taniyama, Y. Tokura, and S. Tarucha, Phys. Rev. Lett. **107**, 146801 (2011).
[6] R. Hanson, L. H. Willems van Beveren, I. T. Vink, J. M. Elzerman, W. J. M. Naber, F. H. L. Koppens, L. P. Kouwenhoven, and L. M. K. Vandersypen, Phys. Rev. Lett. **94**, 196802 (2005).
[7] H. Kosaka, H. Shigyou, Y. Mitsumori, Y. Rikitake, H. Imamura, T. Kutsuwa, K. Arai, and K. Edamatsu, Phys. Rev. Lett. **100**, 096602 (2008).
[8] H. Kosaka, T. Inagaki, Y. Rikitake, H. Imamura, Y. Mitsumori, and K. Edamatsu, Nature (London) **457**, 702 (2009).
[9] W. B. Gao, P. Fallahi, E. Togan, J. Miguel-Sanchez, and A. Imamoglu, Nature (London) **491**, 426 (2012).
[10] K. De Greve, L. Yu, P. L. McMahon, J. S. Pelc, C. M. Natarajan, N. Y. Kim, E. Abe, S. Maier, C. Schneider, M. Kamp, S. Höfling, R. H. Hadfield, A. Forchel, M. M. Fejer, and Y. Yamamoto, Nature (London) **491**, 421 (2012).
[11] J. R. Schaibley, A. P. Burgers, G. A. McCracken, L.-M. Duan, P. R. Berman, D. G. Steel, A. S. Bracker, D. Gammon, and L. J. Sham, Phys. Rev. Lett. **110**, 167401 (2013).
[12] H. Kosaka, D. S. Rao, H. D. Robinson, P. Bandaru, K. Makita, and E. Yablonovitch, Phys. Rev. B **67**, 045104 (2003).
[13] D. S. Rao, T. Szkopek, H. D. Robinson, E. Yablonovitch, and H. W. Jiang, J. Appl. Phys. **98**, 114507 (2005).
[14] J. M. Elzerman, R. Hanson, L. H. W. van Beveren, B. Witkamp, L. M. K. Vandersypen, and L. P. Kouwenhoven, Nature (London) **430**, 431 (2004).
[15] E. Yablonovitch, H. W. Jiang, H. Kosaka, H. D. Robinson, D. S. Rao, and T. Szkopek, Proc. IEEE **91**, 761 (2003).
[16] S. Amasha, K. MacLean, I. P. Radu, D. M. Zumbuhl, M. A. Kastner, M. P. Hanson, and A. C. Gossard, Phys. Rev. Lett. **100**, 046803 (2008).
[17] See Supplemental Material at http://link.aps.org/supplemental/10.1103/PhysRevLett.110.266803 for details on calculations of the aperture transmittance and the trapping efficiency.
[18] L. X. He, K. P. Martin, and R. J. Higgins, Phys. Rev. B **39**, 1808 (1989).
[19] A. C. Johnson, J. R. Petta, J. M. Taylor, A. Yacoby, M. D. Lukin, C. M. Marcus, M. P. Hanson, and A. C. Gossard, Nature (London) **435**, 925 (2005).